Cite this: *INEOS OPEN*, **2023**, *6 (2)*, 55–61
DOI: 10.32931/io2306a

*Received 5 October 2023,*
*Accepted 27 November 2023*

http://ineosopen.org

# POLYDIMETHYLSILOXANES WITH GRAFTED NAPHTHALENE FRAGMENTS: SYNTHESIS AND PROPERTIES

A. S. Belova,[a] D. S. Ionov,[b] D. A. Khanin,[a] and Yu. N. Kononevich*[a]

[a] *Nesmeyanov Institute of Organoelement Compounds, Russian Academy of Sciences, ul. Vavilova 28, str. 1, Moscow, 119334 Russia*
[b] *Photochemistry Center, FSRC "Crystallography and Photonics", Russian Academy of Sciences, ul. Novatorov 7A, str. 1, Moscow, 119421 Russia*

## Abstract

Nowadays, the synthesis and investigation of the properties of new fluorescent polymers based on polysiloxanes and organic fluorophores is an actual topic of research. These polymers find application in various fields of science and technology, in particular, as sensors, fluorescent covers, and optical materials. This work describes the method for obtaining new naphthalene end-capped and side-chain modified polydimethylsiloxanes. The physicochemical, optical, and thermal properties of the resulting polymers are thoroughly studied.

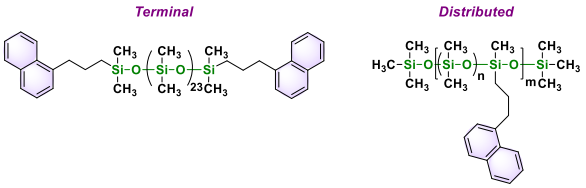


**Key words:** polysiloxanes, naphthalene, hydrosilylation, fluorescence, excimer.

## Introduction

At present, naphthalene and its derivatives comprise the most studied class of organic dyes with valuable optical properties, including the ability to form fluorescent excimers in the excited state [1–12]. The most interesting and promising representatives of these dyes are naphthalene-containing polymers of different architecture since they can be utilized as the materials that are able to change their optical properties under external impact [13–21]. Naphthalene moieties were included in the structures of poly-L-glutamate [14], polyamide [22], and methacrylate [15, 18–21].

Polysiloxanes are remarkable polymers that are widely used in various fields of science and technology as the components of paints [23], electroinsulating materials [24, 25], sealing compounds [26], components of semiconducting materials [27], as well as the optical materials [28]. Excellent biocompatibility of polysiloxanes make them highly useful in cosmetics, pharmaceutics, and medicine [29–33]. Silanes and siloxanes of different structure modified with various fluorophores are very attractive objects for optic, photonic and imaging applications. First of all, this is stipulated by the optical transparency of organosilicon matrices and the ease of their modification with required chromophores. Of particular interest as matrices are polysiloxanes since the developed synthetic methods allow one to modify them over a wide range. In these polymers, the distance between the grafted chromophores could be easily regulated, thus enabling fine-tuning of the optical properties [34–36]. Earlier the multifunctional naphthalene-containing systems based on silane [37], siloxane [38, 39], cyclosiloxane [39–41], silsesquioxane [42], and polysiloxane [43–45] matrices were reported. Therefore, the synthesis of new polysiloxanes with naphthalene substituents and investigation of their properties in the context of development of new promising optical materials is currently an actual topic of research.

Herein, we report the synthesis of new naphthalene end-capped and side-chain modified polydimethylsiloxanes as well as their physicochemical, optical, and thermal properties.

## Results and discussion

In the present work, polydimethylsiloxanes with terminal silylhydride groups (**M1**) and those distributed along the chain (**M2**) were used as silicone matrices for grafting naphthalene fragments (Fig. 1).

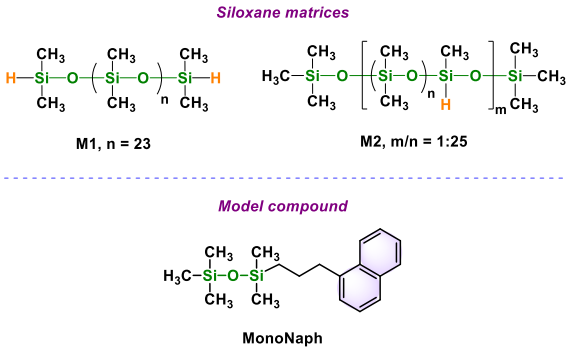


**Figure 1.** Structures of the polysiloxane matrices with terminal silylhydride groups (**M1**) and those distributed along the chain (**M2**), as well as model naphthalene derivative **MonoNaph**.

Polymer **M1** was prepared by the cationic ring-opening polymerization of octamethylcyclotetrasiloxane (D4) using tetramethyldisiloxane as a chain terminator and Amberlyst 15 as a catalyst. Polymer **M2** was synthesized in the same manner from D4 and heptamethylcyclotetrasiloxane using hexamethyldisiloxane as a chain terminator and Amberlyst 15 as a catalyst by the method described earlier [46]. Polysiloxanes

**M1** and **M2** were obtained as colorless oils with the molecular characteristics presented in Table 1.

**Table 1.** Molecular characteristics of **M1**, **M2**, **P1**, and **P2**

| Comp. | $M_n$, kDa | $M_w$, kDa | PDI |
|---|---|---|---|
| **M1** | 2.5 | 4.1 | 1.66 |
| **M2** | 31.8 | 47 | 1.48 |
| **P1** | 3.6 | 5 | 1.39 |
| **P2** | 44.2 | 76 | 1.73 |

1-Allylnaphthalene was used as a functional naphthalene derivative which was prepared by the method described earlier by our research group [39]. **MonoNaph** was used as a model compound for comparison of its optical properties with those of resulting polymers **M1** and **M2** (Fig. 1) [39].

The naphthalene end-capped (**P1**) and side-chain modified (**P2**) polydimethylsiloxanes were obtained by the Pt-catalyzed hydrosilylation in toluene according to Scheme 1 and were purified by preparative gel permeation chromatography (GPC). The reaction course was monitored by NMR spectroscopy and its completion was determined by the disappearance of a signal of the Si–H group. Table 1 lists the molecular characteristics of **P1** and **P2**.

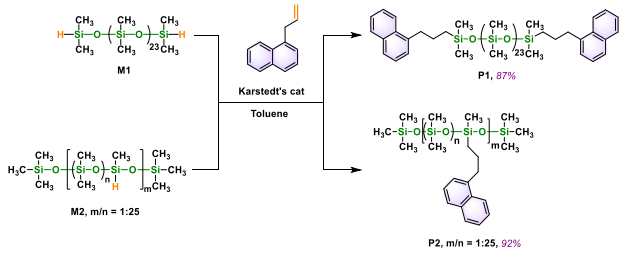


**Scheme 1.** Synthesis of **P1** and **P2**.

The photophysical properties of polymers **P1**, **P2** were studied using electron absorption and steady-state fluorescence spectroscopy (Table 2). Figures 2 and 3 show the normalized absorption and emission spectra of **P1** and **P2** in cyclohexane, chloroform, and ethanol. As can be seen, the absorption and emission spectra of **P1** and **P2** are typical for naphthalene derivatives. However, in the case of the fluorescence spectrum of **P2** in ethanol, a new broad band at 400 nm was detected that can be attributed to the emission of naphthalene excimers. In addition, there was broadening in the absorption spectrum of **P2** in ethanol, which probably corresponds to naphthalene aggregates. This behavior of **P2** in ethanol can be rationalized by the fact that ethanol is a poor solvent for polysiloxanes and promotes the appearance of naphthalene aggregates in solution. At the same time, the corresponding spectra of **P1** do not contain the bands attributed to naphthalene aggregates and excimers. It should be noted that the optical properties of model compound **MonoNaph** in different solvents were studied previously and it was shown that it does not exhibit excimer fluorescence in dilute solutions [39].

The absorption spectra of **P1** and **P2** in the condensed state are typical for naphthalene derivatives and **P1**-**P2** in different solvents (Fig. 4, top). The fluorescence spectra of **P1**, **P2**, and **MonoNaph** in the condensed state, in addition to the emission of a naphthalene moiety, show an intense red-shifted band of the excimer emission (Fig. 4, bottom). As can see from Fig. 4, the

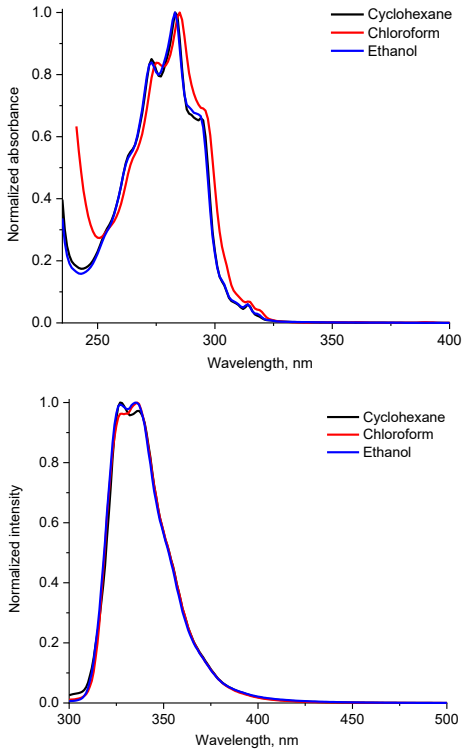


**Figure 2.** Normalized absorption (top) and fluorescence (bottom) spectra of **P1** in different solvents at room temperature ($\lambda_{ex}$ = 270 nm, $c$ = 1 μM).

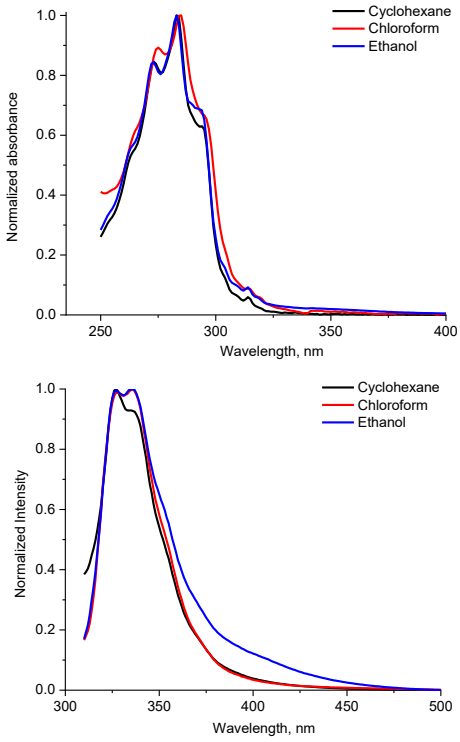


**Figure 3.** Normalized absorption (top) and fluorescence (bottom) spectra of **P2** in different solvents at room temperature ($\lambda_{ex}$ = 270 nm, $c$ = 1 μM).

content of excimers for **MonoNaph** is higher than in the case of polymers **P1** and **P2**, which can be associated with the higher degree of freedom in **MonoNaph** to form excimers in the excited state.

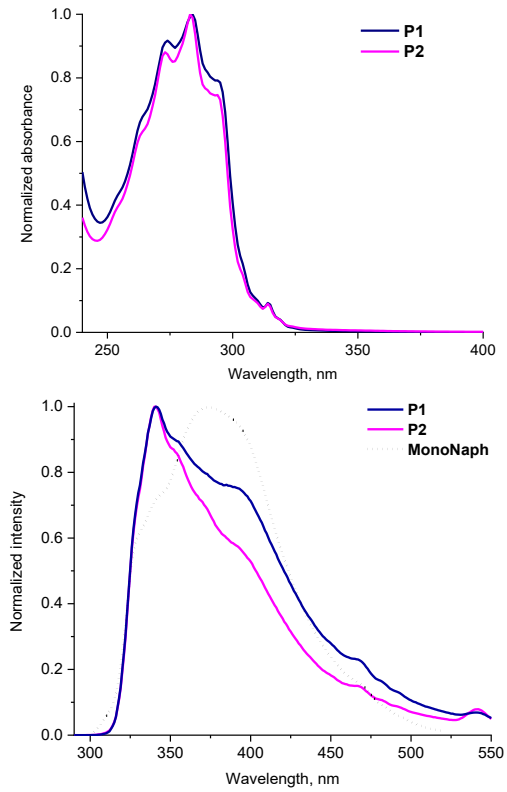


**Figure 4.** Normalized absorption spectra of **P1**, **P2** (top) and fluorescence spectra of **P1**, **P2**, and **MonoNaph** (bottom) in the condensed state (viscous liquids, $\lambda_{ex}$ = 270 nm).

To quantify the intramolecular excimers in dilute solutions of **P1** and **P2**, the corresponding fluorescence spectra were compared with those of **MonoNaph** measured in the same solvents. Then, the excimer/monomer ratio was found using the following equation:

$$\frac{I_{ex}}{I_m} = \frac{I_{ex} - I_{MonoNaph400}}{I_{norm}}, \quad (1)$$

where $I_{ex}$ is the intensity of the excimer emission; $I_m$ is the intensity of the monomer emission; $I_{ex400}$ is the intensity at 400 nm in the normalized emission spectra of **P1** and **P2** (400 nm was selected as the wavelength close to the excimer emission maximum); $I_{MonoNaph400}$ is the intensity at 400 nm in the normalized emission spectra of **MonoNaph**; $I_{norm}$ is the intensity used to normalize the emission spectra at the maximum [47]. As can be seen from the data summarized in Table 2, the highest values of $I_{ex}/I_m$ are observed in the case of **P2** in ethanol.

**Table 2.** Optical properties of **P1** and **P2** in different solvents

| Comp. | Solvent | $\lambda_{abs}$, nm | $\lambda_{em}$, nm | $\Phi_f$[a] | $I_{ex}/I_m$ |
|---|---|---|---|---|---|
| **P1** | Cyclohexane | 283 | 327 (336) | 0.43 | 0.00 |
| | Chloroform | 285 | 336 (327) | 0.06 | 0.00 |
| | Ethanol | 283 | 327 (335) | 0.49 | 0.00 |
| **P2** | Cyclohexane | 283 | 327 (335) | 0.44 | 0.02 |
| | Chloroform | 285 | 336 (328) | 0.09 | 0.01 |
| | Ethanol | 283 | 327 (335) | n.d. | 0.10 |

$\lambda_{abs}$ is the absorption wavelength; $\lambda_{em}$ is the emission wavelength; $\Phi_f$ is the fluorescence quantum yield; the wavelengths of the second fluorescence peaks are given in parentheses;

[a] naphthalene was used as a standard for calculating the quantum yield ($\Phi_f$ = 0.23; argon-purged solution in cyclohexane).

The fluorescence decay curves of **P1** and **P2** solutions in aerated and deaerated cyclohexane, chloroform, and ethanol registered at 335 nm are depicted in Fig. 5.

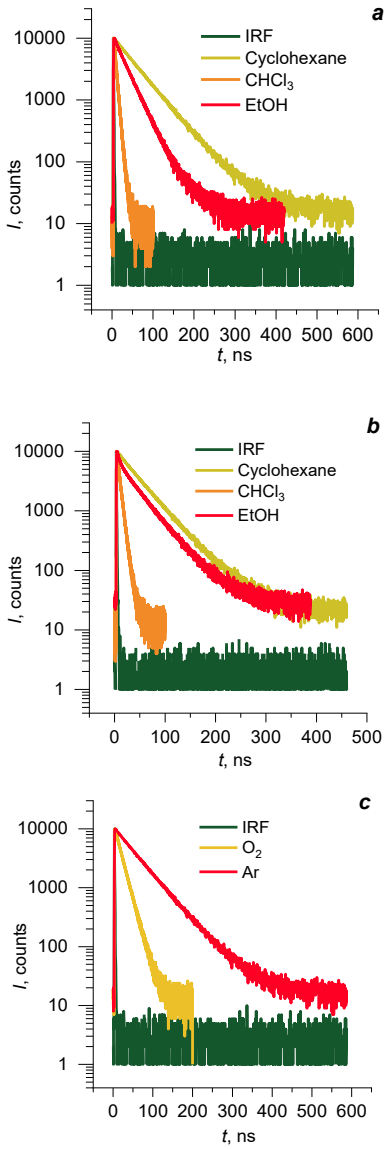


**Figure 5.** Fluorescence decay kinetics of **P1** (***a***) and **P2** (***b***) in cyclohexane, chloroform, and ethanol. The comparison of fluorescence decays of **P1** in aerated and argon-purged cyclohexane (***c***). All kinetic curves were obtained at the wavelength of 335 nm ($\lambda_{ex}$ = 275 nm).

The resulting curves are non-monoexponential and require at least two exponential terms for satisfactory ($\chi^2$ < 1.3) fitting. The fitting results are presented in Table 3. The biexponential decay seems to attribute to the interaction of fluorophore moieties during the excimer formation process. The fluorescence of **P1** and **P2** is effectively quenched by oxygen. After oxygen removal, the decay lifetime in cyclohexane becomes almost three times longer, as can be seen in Fig. 5c.

Figures 6 and 7 show the fluorescence decay kinetics of **P1** and **P2** in the condensed state measured at 335 and 420 nm in air and argon. The results of global fitting of the data obtained are presented in Table 4. It should be noted that all the kinetics include a significant contribution of the fast component ($\tau$ < 50 ps), which cannot be distinguished from the instrument response

**Table 3.** Results of approximation of the fluorescence decay kinetics of the **P1** and **P2** solutions in cyclohexane, chloroform, and ethanol obtained at 335 nm ($\lambda_{ex}$ = 275 nm)

| Sample | | Air | | | Ar | | |
|---|---|---|---|---|---|---|---|
| | | $\tau$, ns | A, % | $\chi^2$ | $\tau$, ns | A, % | $\chi^2$ |
| **P1** | $C_6H_{12}$ | 16.8 | 92 | 1.13 | 55.8 | 94 | 1.06 |
| | | 4.7 | 8 | | 11.5 | 6 | |
| | $CHCl_3$ | 4.5 | 82 | 1.28 | 5.6 | 82 | 1.28 |
| | | 0.9 | 18 | | 1.6 | 18 | |
| | EtOH | 16.7 | 89 | 1.10 | 30.6 | 88 | 1.27 |
| | | 5.9 | 11 | | 9.0 | 12 | |
| **P2** | $C_6H_{12}$ | 17.6 | 90 | 1.11 | 47.9 | 72 | 1.13 |
| | | 5.8 | 10 | | 28.7 | 28 | |
| | $CHCl_3$ | 4.9 | 74 | 1.29 | 6.0 | 75 | 1.38 |
| | | 0.9 | 26 | | 1.3 | 25 | |
| | EtOH | 17.8 | 55 | 1.20 | 40.3 | 57 | 1.21 |
| | | 3.9 | 45 | | 5.3 | 43 | |

function (IRF). This component can be associated both with fast processes and with scattered light from the excitation source. During fitting procedure, the component in question was classified as scattered light. The resulting kinetic curves are best approximated by a model with three exponential terms ($\chi^2 \leq$ 1.3). At a wavelength of 420 nm, the fitting results contain exponential terms with a negative amplitude, which indicates the occurrence of rearrangement of the relative fluorophore positions in the excited state. The three exponential terms are presumably observed due to the presence of dimers and excimers of various structures in polymers. Their structural rearrangement into the most favorable geometry, corresponding to the excimers in solutions, is complicated by the interaction with the polymer chains. In argon, the lifetime of fluorophores increases due to reduction of effective quenching of the excited states by oxygen.

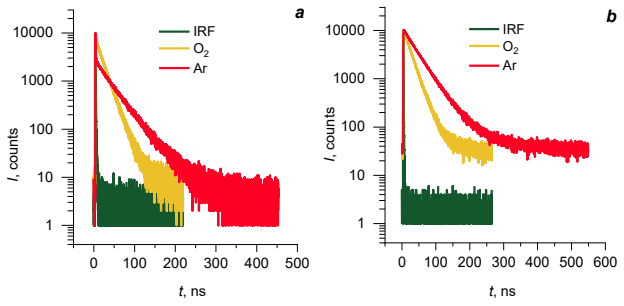


**Figure 6.** Fluorescence decay kinetics of polymer **P1** at 335 (***a***) and 420 nm (***b***) ($\lambda_{ex}$ = 275 nm).

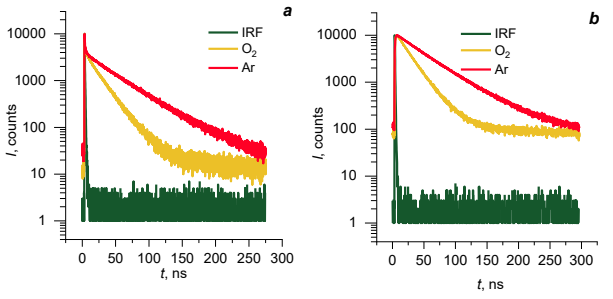


**Figure 7.** Fluorescence decay kinetics of polymer **P2** at 335 (***a***) and 420 nm (***b***) ($\lambda_{ex}$ = 275 nm).

**Table 4**. Results of global approximation of the fluorescence decay kinetics of **P1** and **P2** in the condensed state ($\lambda_{ex}$ = 275 nm)

| Sample | | $\tau$, ns | $A_{\lambda = 335\ nm}$, a.u. | $A_{\lambda = 420\ nm}$, a.u. | $\chi^2$ |
|---|---|---|---|---|---|
| **P1** | $O_2$ | 19.2 | 5.5 | 18.5 | 1.15 |
| | | 11.3 | 2.6 | 4.7 | |
| | | 0.78 | 4.8 | –7.6 | |
| | Ar | 43.4 | 1.6 | 8.0 | 1.31 |
| | | 26.5 | 1.1 | 4.5 | |
| | | 1.51 | 1.7 | –0.4 | |
| **P2** | $O_2$ | 43.3 | 0.1 | 1.2 | 1.16 |
| | | 20.4 | 3.7 | –2.6 | |
| | | 1.75 | 1.9 | –10.0 | |
| | Ar | 49.81 | 3.1 | 18.5 | 1.08 |
| | | 20.0 | 0.8 | 2.3 | |
| | | 1.53 | 1.8 | –11.8 | |

The thermal properties of polymers **P1** and **P2** were investigated by thermogravimetric analysis (TGA) and differential scanning calorimetry (DSC) (Figs. 8, 9, Tables 5, 6). It was found that the introduction of terminal naphthalene fragments into polysiloxane **P1** leads to an increase in the thermal stability up to 305 °C in air and 300 °C in argon. At the same time, **P2** show thermal stability similar to that of **M2**. The mass loss at a relatively low temperature in the case of **M1** is obviously associated with the sample evaporation. Furthermore, it should be mentioned that the introduction of naphthalene fragments into the polysiloxanes leads to the loss of crystallization of the latter.

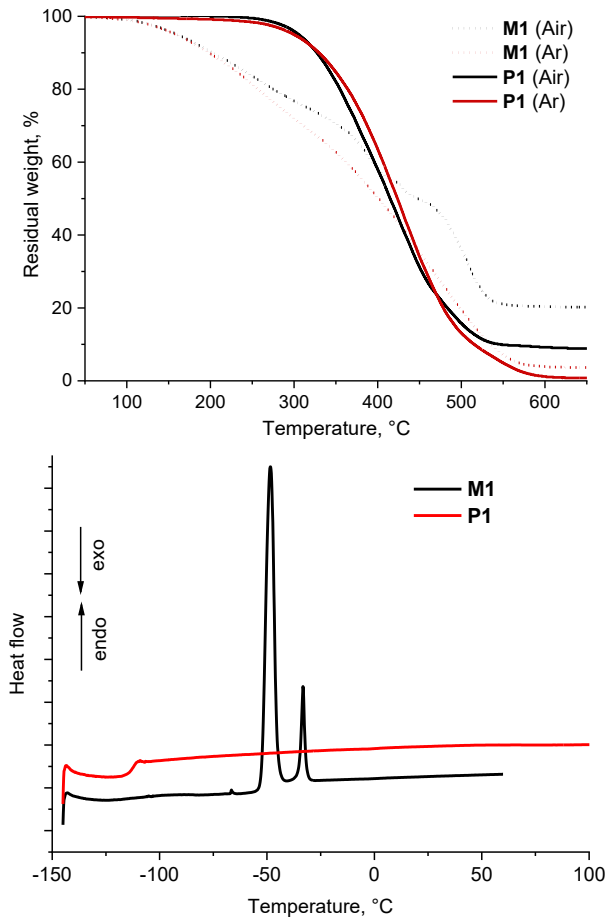


**Figure 8.** TGA (top) and DSC (bottom) curves for **M1** and **P1**.

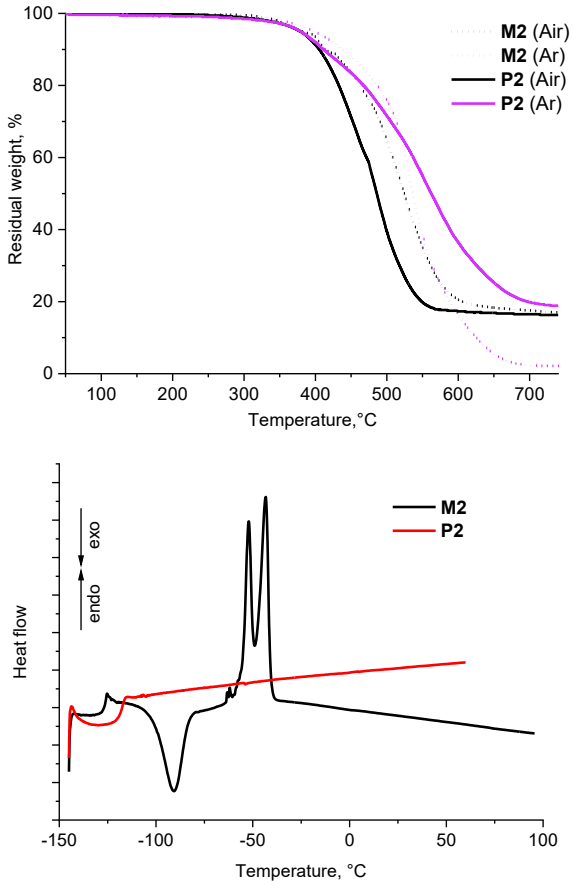


**Figure 9.** TGA (top) and DSC (bottom) curves for **M2** and **P2**.

**Table 5.** TGA analysis data for polymers **M1**, **M2**, **P1**, and **P2**

| Comp. | $T_d^{5\%}$, °C | | Residue after decomposition, % | |
|---|---|---|---|---|
| | Air | Ar | Air | Ar |
| **M1** | 160 | 158 | 20 | 4 |
| **M2** | 382 | 398 | 17 | 2 |
| **P1** | 305 | 300 | 9 | 0 |
| **P2** | 378 | 379 | 16 | 18 |

$T_d^{5\%}$ is the temperature at which a weight loss of 5% was detected.

**Table 6.** DSC analysis data for polymers **M1**, **M2**, **P1**, and **P2**

| Comp. | $T_g$, °C | $T_{cc}$, °C | $\Delta H_{cc}$, J/g | $T_{m1}$, °C | $\Delta H_{m1}$, J/g | $T_{m2}$, °C | $\Delta H_{m2}$, J/g |
|---|---|---|---|---|---|---|---|
| **M1** | – | – | – | –48.5 | 39.9 | –33.2 | 5.7 |
| **M2** | –127 | –90.5 | 16.6 | –52 | 13.8 | –43 | 16.9 |
| **P1** | –112 | – | – | – | – | – | – |
| **P2** | –118 | – | – | – | – | – | – |

$T_g$ is the glass transition temperature.

## Experimental section

### General remarks

Octamethylcyclotetrasiloxane, heptamethylcyclotetrasiloxane, hexamethyldisiloxane, tetramethyldisiloxane, and Amberlyst 15 were purchased from ABCR. 1-Allylnaphthalene was prepared by the previously described procedure [39]. Platinum(0)-1,3-divinyl-1,1,3,3-tetramethyldisiloxane complex solution (in xylene, Pt-2%) was purchased from Sigma-Aldrich. All chemicals were used without further purification. Toluene was distilled from $CaH_2$. The $^1$H, $^{13}$C, and $^{29}$Si NMR spectra were recorded on a Bruker Avance II spectrometer (400 MHz, Germany). The chemical shifts for the $^1$H NMR spectra are reported relative to chloroform ($\delta$ = 7.25 ppm). The IR spectra were recorded on a Shimadzu IRTracer-100 IR FTIR spectrometer (Japan). The GPC analyses were performed in toluene (1 mL/min) using a Shimadzu Prominent system equipped with an RID-20A refractive index detector. The GPC columns (Phenogel) were calibrated with polystyrene standards (PSS). The absorption spectra were recorded on a Shimadzu UV-1900 spectrophotometer (Japan). The fluorescence spectra in solution and in the condensed state were measured on a Shimadzu RF-6000 spectrofluorophotometer (Japan). Spectroscopic grade solvents (Aldrich) were used in UV-vis absorption and fluorescence measurements. To measure the optical properties in solution, the quartz cells with an optical path length of 10 mm were used. The optical densities were typically between 0.7 and 0.9 for the absorption measurements and around 0.03–0.09 for the fluorescence measurements ($c$ = 1 μM). The optical properties in the condensed state were measured using films with a thickness of about 200–500 μm. The fluorescence quantum yields were determined using naphthalene as a reference. The fluorescence decay curves were obtained with a Picoquant Fluotime 300 spectrofluorometer. PLS-270 was used as an excitation source ($\lambda_{ex}$ = 275 nm). Filter HOYA UV-30 was installed before an entrance slit of the emission monochromator to reduce scattered excitation light. The data fitting was performed using the Easytau2 (Picoquant) software. The TGA studies were performed on a Shimadzu DTG-60H instrument (Japan) using 5 mg samples at a heating rate of 10 °C/min in air or argon. The temperature at which a weight loss of 5% was detected was considered to be the decomposition onset temperature. The DSC measurements were performed on a Mettler-Toledo DSC-3 calorimeter (Switzerland) at a heating rate of 10 °C/min in an argon atmosphere.

### Syntheses

**Polysiloxane with the end-capped Si–H groups (M1)**. A mixture of octamethylcyclotetrasiloxane (0.160 mol), tetramethyldisiloxane (0.032 mol), and Amberlyst 15 (0.1 g) was stirred at 80 °C for 24 h. After the reaction completion, the resulting mixture was cooled down to room temperature. Amberlyst 15 was filtered off. Then, the filtrate was dried in a vacuum oven (1 mbar) at 100 °C for 6 h. Polymer **M1** was obtained as a colorless oil. Yield: 72%. $M_n$ = 2.5 kDa, $M_w$ = 4.1 kDa, PDI = 1.66. $^1$H NMR (400 MHz, $CDCl_3$): $\delta$ 0.06 (s, 141H, $SiCH_3$), 0.18 (d, 12H, $J$ = 2.7 Hz, $SiCH_3$), 4.70 (m, 2H, SiH) ppm. $^{13}$C NMR (101 MHz, $CDCl_3$): $\delta$ 0.7, 0.9, 1.0 ppm. $^{29}$Si NMR (79 MHz, $CDCl_3$): $\delta$ –21.88, –21.76, –19.80, –6.87 ppm. IR (KBr, $\nu$/cm$^{-1}$): 2963, 2905, 2128, 1413, 1261, 1093, 1023, 914, 864, 798, 704, 660.

**Polysiloxane with the end-capped naphthalene fragments (P1)**. A solution of 1-allylnaphthalene (1.630 mmol), polymer **M1** (0.545 mmol), and Karstedt's catalyst (0.03 mL, 0.3 mol % [Pt]) in dry toluene (10 mL) was stirred at room temperature in an argon atmosphere for 24 h. After the reaction completion, the solvent was removed under vacuum. Polymer **P1** was purified by GPC. Yield: 87%. $M_n$ = 3.6 kDa, $M_w$ = 5 kDa, PDI = 1.39. $^1$H

NMR (400 MHz, $CDCl_3$): $\delta$ 0.08 (s, 151H, $SiCH_3$), 0.71 (m, 2H, $SiCH_2$), 1.80 (m, 2H, $CH_2$), 3.09 (m, 2H, $CH_2$), 7.31 (d, 2H, Ar), 7.40 (t, 2H, Ar), 7.48 (m, 4H, Ar), 7.72 (d, 2H, Ar), 7.85 (d, 2H, Ar), 8.04 (d, 2H, Ar) ppm. $^{13}$C NMR (101 MHz, $CDCl_3$): $\delta$ –0.65, 0.20, 0.32, 17.80, 23.90, 36.01, 123.06, 124.48, 124.65, 124.76, 125.11, 125.56, 127.85, 133.02, 137.95 ppm. $^{29}$Si NMR (79 MHz, $CDCl_3$): $\delta$ –21.91, 7.36 ppm. IR (KBr, $\nu$/cm$^{-1}$): 3096, 3062, 3048, 2962, 2905, 2873, 2797, 2662, 2499, 1943, 1597, 1511, 1445, 1412, 1400, 1260, 1093, 1020, 863, 796, 703, 662, 504.

**Polysiloxane with the side-chain distributed naphthalene fragments (P2)**. A solution of 1-allylnaphthalene (0.66 mmol), polymer **M2** (0.33 mol), and Karstedt's catalyst (0.03 mL, 0.3 mol % [Pt]) in dry toluene (10 mL) was stirred at room temperature in an argon atmosphere for 24 h. After the reaction completion, the solvent was removed under vacuum. Polymer **P1** was purified by GPC. Yield: 92%. $M_n$ = 44.2 kDa, $M_w$ = 76.7 kDa, PDI = 1.73. $^1$H NMR (400 MHz, $CDCl_3$): $\delta$ 0.06 (s, 176H, $SiCH_3$), 0.66 (m, 2H, $SiCH_2$), 1.80 (m, 2H, $CH_2$), 3.06 (m, 2H, $CH_2$), 7.29 (d, 2H, Ar), 7.36 (t, 2H, Ar), 7.45 (m, 4H, Ar), 7.68 (d, 2H, Ar), 7.82 (d, 2H, Ar), 8.02 (d, 2H, Ar) ppm. $^{13}$C NMR (101 MHz, $CDCl_3$): $\delta$ 0.8, 1.2, 1.6, 18.0, 24.5, 36.8, 124.1, 125.5, 125.6, 125.7, 126.1, 126.5, 128.8 ppm. $^{29}$Si NMR (79 MHz, $CDCl_3$): $\delta$ –50.01, –21.91 ppm. IR (KBr, $\nu$/cm$^{-1}$): 3097, 3063, 3048, 2963, 2906, 2799, 2663, 2500, 2052, 1944, 1598, 1512, 1446, 1412, 1400, 1261, 1095, 1020, 864, 799, 703, 687, 662, 499.

## Conclusions

In summary, the method for obtaining new naphthalene end-capped and side-chain modified polydimethylsiloxanes was described. The investigation of the optical properties using electron absorption and steady-state fluorescence spectroscopy revealed that both of the resulting polymers exhibit excimer fluorescence in the condensed state. The thermal properties were studied by thermogravimetric analysis and differential scanning calorimetry. It was shown that the introduction of terminal naphthalene fragments into the polysiloxane leads to an increase in the thermal stability up to 305 °C in air and 300 °C in argon. The introduction of the naphthalene fragments into the polysiloxanes leads to the loss of crystallization of the latter.

## Acknowledgements

The spectroscopic studies were performed with financial support from the Ministry of Science and Higher Education of the Russian Federation (agreement no. 075-00277-24-00) using the equipment of the Center for Molecular Composition Studies of INEOS RAS. The fluorescence lifetime measurements were performed using the equipment of the Shared Research Center "Structural diagnostics of materials" of FSRC "Crystallography and Photonics" RAS within the state assignment FSRC "Crystallography and Photonics" RAS.

## Corresponding author

* E-mail: kononevich.yuriy@gmail.com (Yu. N. Kononevich)

## References

1. P. F. Jones, M. Nicol, *J. Chem. Phys.*, **1965**, *43*, 3759–3760. DOI: 10.1063/1.1696547
2. P. F. Jones, M. Nicol, *J. Chem. Phys.*, **1968**, *48*, 5457–5464. DOI: 10.1063/1.1668239
3. C. Agarwal, E. Prasad, *RSC Adv.*, **2014**, *4*, 8015–8022. DOI: 10.1039/c3ra45510f
4. X. Xiang, D. Wang, Y. Guo, W. Liu, W. Qin, *Photochem. Photobiol. Sci.*, **2013**, *12*, 1232–1241. DOI: 10.1039/c3pp00007a
5. P. F. Jones, M. Nicol, *J. Chem. Phys.*, **1968**, *48*, 5440–5447. DOI: 10.1063/1.1668237
6. M. Nicol, M. Vernon, J. T. Woo, *J. Chem. Phys.*, **1975**, *63*, 1992–1999. DOI: 10.1063/1.431535
7. K. Uchida, M. Tanaka, M. Tomura, *J. Lumin.*, **1979**, *20*, 409–414. DOI: 10.1016/0022-2313(79)90012-7
8. J. B. Birks, J. B. Aladekomo, *Spectrochim. Acta*, **1964**, *20*, 15–21. DOI: 10.1016/0371-1951(64)80196-X
9. B. Narayan, K. Nagura, T. Takaya, K. Iwata, A. Shinohara, H. Shinmori, H. Wang, Q. Li, X. Sun, H. Li, S. Ishihara, T. Nakanishi, *Phys. Chem. Chem. Phys.*, **2018**, *20*, 2970–2975. DOI: 10.1039/C7CP05584F
10. L. Mohanambe, S. Vasudevan, *J. Phys. Chem. B*, **2005**, *109*, 22523–22529. DOI: 10.1021/jp053925f
11. M. Vera, H. Santacruz Ortega, M. Inoue, L. Machi, *Supramol. Chem.*, **2019**, *31*, 336–348. DOI: 10.1080/10610278.2019.1588971
12. S. Adhikari, S. Mandal, A. Ghosh, S. Guria, D. Das, *Dalton Trans.*, **2015**, *44*, 14388–14393. DOI: 10.1039/C5DT02146D
13. Y. Itoh, M. Inoue, *Eur. Polym. J.*, **2000**, *36*, 2605–2610. DOI: 10.1016/S0014-3057(00)00052-5
14. H. Itagaki, K. Sugiura, H. Sato, *Macromol. Chem. Phys.*, **2001**, *202*, 90–96. DOI: 10.1002/1521-3935(20010101)202:1<90::AID-MACP90>3.0.CO;2-H
15. L. Cheng, G. Wang, M. A. Winnik, *Polymer*, **1990**, *31*, 1611–1614. DOI: 10.1016/0032-3861(90)90176-Y
16. F. Mendicuti, B. Patel, W. L. Mattice, *Polymer*, **1990**, *31*, 453–457. DOI: 10.1016/0032-3861(90)90384-B
17. R. F. Reid, I. Soutar, *J. Polym. Sci., Polym. Phys. Ed.*, **1978**, *16*, 231–244. DOI: 10.1002/pol.1978.180160205
18. D. Phillips, A. J. Roberts, I. Soutar, *Polymer*, **1981**, *22*, 293–298. DOI: 10.1016/0032-3861(81)90038-0
19. R. F. Reid, I. Soutar, *J. Polym. Sci., Polym. Phys. Ed.*, **1980**, *18*, 457–467. DOI: 10.1002/pol.1980.180180306
20. R. A. Anderson, R. F. Reid, I. Soutar, *Eur. Polym. J.*, **1979**, *15*, 925–929. DOI: 10.1016/0014-3057(79)90230-1
21. S. Nishimoto, K. Yamamoto, T. Kagiya, *Macromolecules*, **1982**, *15*, 1180–1185. DOI: 10.1021/ma00232a043
22. J. A. Ibemesi, J. B. Kinsinger, M. A. El-Bayoumi, *J. Polym. Sci., Polym. Chem. Ed.*, **1980**, *18*, 879–890. DOI: 10.1002/pol.1980.170180309
23. S. Ahmad, A. P. Gupta, E. Sharmin, M. Alam, S. K. Pandey, *Prog. Org. Coat.*, **2005**, *54*, 248–255. DOI: 10.1016/j.porgcoat.2005.06.013
24. J. Hong, J. Lee, D. Jung, S. E. Shim, *Thermochim. Acta*, **2011**, *512*, 34–39. DOI: 10.1016/j.tca.2010.08.019
25. S. Simmons, M. Shah, J. Mackevich, R. J. Chang, *IEEE Electr. Insul. Mag.*, **1997**, *13*, 25–32. DOI: 10.1109/57.620515
26. F. de Buyl, *Int. J. Adhes. Adhes.*, **2001**, *21*, 411–422. DOI: 10.1016/S0143-7496(01)00018-5
27. S. C. Surita, B. Tansel, *Ecotoxicol. Environ. Saf.*, **2014**, *102*, 79–83. DOI: 10.1016/j.ecoenv.2014.01.012
28. C. E. Brunchi, A. Filimon, M. Cazacu, S. Ioan, *High Perform. Polym.*, **2009**, *21*, 31–47. DOI: 10.1177/0954008308088737
29. J. Curtis, A. Colas, in: *Biomaterials Science (Third Ed.)*, B. D. Ratner, A. S. Hoffman, F. J. Schoen, J. E. Lemons, (Eds.), *Acad. Press*, **2013**, ch. II.5.18, pp. 1106–1116. DOI: 10.1016/B978-0-08-087780-8.00107-8

30. B. D. Ratner, A. S. Hoffman, in: *Biomaterials Science (Third Ed.)*, B. D. Ratner, A. S. Hoffman, F. J. Schoen, J. E. Lemons, (Eds.), *Acad. Press*, **2013**, ch. I.2.10, pp. 241–247. DOI: 10.1016/B978-0-08-087780-8.00025-5
31. T. R. Neu, H. C. Van der Mei, H. J. Busscher, F. Dijk, G. J. Verkerke, *Biomaterials*, **1993**, *14*, 459–464. DOI: 10.1016/0142-9612(93)90149-V
32. M. J. Whitford, *Biomaterials*, **1984**, *5*, 298–300. DOI: 10.1016/0142-9612(84)90077-2
33. B. Ustbas, D. Kilic, A. Bozkurt, M. E. Aribal, O. Akbulut, *Ultrasonics*, **2018**, *88*, 9–15. DOI: 10.1016/j.ultras.2018.03.001
34. A. S. Belova, A. G. Khchoyan, T. M. Il'ina, Y. N. Kononevich, D. S. Ionov, V. A. Sazhnikov, D. A. Khanin, G. G. Nikiforova, V. G. Vasil'ev, A. M. Muzafarov, *Polymers*, **2022**, *14*, 5075. DOI: 10.3390/polym14235075
35. A. S. Belova, Y. N. Kononevich, D. S. Ionov, V. A. Sazhnikov, A. D. Volodin, A. A. Korlyukov, P. V. Dorovatovskii, M. V. Alfimov, A. M. Muzafarov, *Dyes Pigm.*, **2023**, *208*, 110852. DOI: 10.1016/j.dyepig.2022.110852
36. Y. N. Kononevich, A. S. Belova, V. A. Sazhnikov, A. A. Safonov, D. S. Ionov, A. D. Volodin, A. A. Korlyukov, A. M. Muzafarov, *Tetrahedron Lett.*, **2020**, *61*, 152176. DOI: 10.1016/j.tetlet.2020.152176
37. T. Karatsu, T. Shibata, A. Nishigaki, A. Kitamura, Y. Hatanaka, Y. Nishimura, S.-i. Sato, I. Yamazaki, *J. Phys. Chem. B*, **2003**, *107*, 12184–12191. DOI: 10.1021/jp0355760
38. K. Imai, S. Hatano, A. Kimoto, J. Abe, Y. Tamai, N. Nemoto, *Tetrahedron*, **2010**, *66*, 8012–8017. DOI: 10.1016/j.tet.2010.08.010
39. A. S. Belova, Yu. N. Kononevich, V. A. Sazhnikov, A. A. Safonov, D. S. Ionov, A. A. Anisimov, O. I. Shchegolikhina, M. V. Alfimov, A. M. Muzafarov, *Tetrahedron*, **2021**, *93*, 132287. DOI: 10.1016/j.tet.2021.132287
40. M. Laird, C. Carcel, M. Unno, J. R. Bartlett, M. Wong Chi Man, *Molecules*, **2022**, *27*, 7680. DOI: 10.3390/molecules27227680
41. S.-i. Kondo, S. Abe, H. Katagiri, *Dyes Pigm.*, **2023**, *217*, 111394. DOI: 10.1016/j.dyepig.2023.111394
42. H. Narikiyo, M. Gon, K. Tanaka, Y. Chujo, *Mater. Chem. Front.*, **2018**, *2*, 1449–1455. DOI: 10.1039/C8QM00181B
43. J. Sun, H. Tang, J. Jiang, X. Zhou, P. Xie, R. Zhang, P.-F. Fu, *J. Polym. Sci., Part A: Polym. Chem.*, **2003**, *41*, 636–644. DOI: 10.1002/pola.10607
44. S. O. Hwang, A. S. Lee, J. Y. Lee, S.-H. Park, K. I. Jung, H. W. Jung, J.-H. Lee, *Prog. Org. Coat.*, **2018**, *121*, 105–111. DOI: 10.1016/j.porgcoat.2018.04.022
45. M. Briesenick, M. Gallei, G. Kickelbick, *Macromolecules*, **2022**, *55*, 4675–4691. DOI: 10.1021/acs.macromol.2c00265
46. E. E. Kim, Y. N. Kononevich, Y. S. Dyuzhikova, D. S. Ionov, D. A. Khanin, G. G. Nikiforova, O. I. Shchegolikhina, V. G. Vasil'ev, A. M. Muzafarov, *Polymers*, **2022**, *14*, 2554. DOI: 10.3390/polym14132554
47. F. Mendicuti, B. Patel, W. L. Mattice, *Polymer*, **1990**, *31*, 453–457. DOI: 10.1016/0032-3861(90)90384-B